2010

Modeling the effect of vegetation of the accumulation and melting of snow

Vinod Mahat

David G. Tarboton

MODELING THE EFFECT OF VEGETATION OF THE ACCUMULATION AND MELTING OF SNOW

Vinod Mahat[1] and David G. Tarboton[1]

ABSTRACT

This work investigates the variability of snow accumulation and differences in the timing of melt and sublimation between open (grass/shrubs) and forest (conifer/deciduous) locations at a mountain study site in the Western US, using a combination of field observations and modeling. Observations include continuous automated climate and snow depth measurements supported by periodic field measurements of snow water equivalent and temperature in four different vegetation classes (grass, shrubs, coniferous forest, deciduous forest) at the TW Daniel Experimental Forest located 30 miles N-E of Logan. The Utah Energy Balance physically based snowmelt model, was enhanced by adding new parameterizations of: i) snow interception and unloading; ii) transmission of radiation through the canopy; and iii) atmospheric transport of heat and water vapor between the snow on the ground, intercepted snow in the canopy and the atmosphere above; to better simulate snow processes in forested areas. The enhanced model was evaluated by comparing model simulations of meteorological conditions (temperature, wind, radiation) and snow properties (water equivalent, depth, temperature) in and beneath the canopy with observations. Observations showed approximately 10 to 20% more snow accumulation in open areas compared to forest areas. Ablation rates were also found to be higher in open areas than in forest areas. In comparison to coniferous forest, deciduous forest had high rates of accumulation and ablation. The model performed well in representing these effects based on inputs such as canopy height, canopy coverage, leaf area index and leaf orientation; thereby improving our ability to simulate and predict snow processes across heterogeneous watersheds. (KEYWORDS: snow accumulation, melt timing, sublimation, interception, snowmelt)

INTRODUCTION

Snow accumulation, melt and sublimation processes are different for open and forest sites. Vegetation and land cover influences snow processes making it difficult to predict snowmelt which is responsible for water supply. The processes of snow accumulation and melt in open areas are well understood for a range of climates and represented in numerical models (Anderson,1976; Price and Dunne, 1976; Jordan, 1991; Marks et al., 1992; Wigmosta et al., 1994; Tarboton and Luce, 1996). Prediction of the evolution of snow packs in forested areas is more complex (Storck et al. 2002). The forest canopy intercepts snow fall, attenuates radiation, and modifies the turbulent exchanges of energy and water vapor between snow in and under the canopy and the atmosphere, thereby affecting snow accumulation and melt.

Radiation is the main driver for the energy fluxes involved in snow melt and sublimation. There have been several studies conducted to understand the transmission and distribution of radiation through and within the canopy. These studies include bi-layer (dual source) models (e.g. Nijssen and Lettenmaier, 1999; Ellis and Pomeroy, 2007; Shuttleworth and Wallace, 1985) and multiple-layer canopy models (e.g. Choudhury and Monteith, 1988; Flerchinger et al., 1998; Norman, 1979; Bonan, 1991). In a multiple-layer canopy model, the energy balance is solved for each canopy layer while in bi-layer models the whole canopy is represented as a single layer and the energy balance is solved for the canopy and the surface layer only.

Some prior studies have used a single bulk resistance to estimate the turbulent heat and mass transfer from a forest treating the canopy and the underlying surface as a single layer (Andreadis et al., 2009; Marks et al., 1998; Marks et al., 2008). However these models do not consider the separate energy and mass transfers that occur to and from the canopy and the underlying snow and air above. Representation of such processes requires at least a two layer model to separately represent in-canopy and above canopy turbulent flux exchanges (e.g. Sanchez et al., 2009; Bonan, 1991; Dolman, 1993; Wigmosta et al., 1994).

Snow falling on a vegetation canopy is partitioned into interception by the canopy and throughfall to the ground (Hedstrom and Pomeroy, 1998). Intercepted snow may sublimate (Lundberg et al., 1998; Lundberg and Halldin, 1994), unload as mass (Mackay and Barlett, 2006) or melt within the canopy. Sublimation reduces the amount of

Paper presented Western Snow Conference 2010
[1] Department of Civil and Environmental Engineering, USU, Logan, UT

the ground. A significant fraction of total annual snowfall can be intercepted by the vegetation canopy and lost to sublimation (Storck et al., 2002; Molotch et al., 2007; Hedstrom and Pomeroy, 1998; Andreadis et al., 2009). Commonly used snowmelt models do not represent these canopy interception processes, a shortcoming that inhibits their ability to physically predict snowmelt water supply in forested areas where interception/sublimation processes are important (Pomeroy et al., 1998; Lundberg et al., 1998; Nakai et al., 1999; Andreadis et al., 2009).

The purpose of this study is to develop a physically based snowmelt model that comprehensively describes the physical processes that control snow accumulation, melt and sublimation in open as well as forested areas. Much of the focus is on the impact of the vegetation canopy on snow processes. We use a two layer model to distinguish between snow accumulated on the ground surface, either beneath a canopy or in the open, and canopy snow that is held above the surface on vegetation after having been intercepted. A more detailed multi-layer model would more fully represent the canopy hydrological processes, but there is a danger of over parameterization that leads to uncertainty in prediction where the data required for specification of the parameters for each layer may not be available. In this paper we have therefore evaluated the addition of a single canopy layer to the Utah Energy Balance (UEB) model (Tarboton et al., 1995; Tarboton and Luce, 1996) to provide parameterizations for canopy processes (radiation transmission, turbulent energy flux and interception).

STUDY SITE AND DATA COLLECTION

Data collection and field measurements were carried out at the TW Daniel Experimental Forest (TWDEF) located about 30 miles North–East of Logan, Utah. TWDEF comprises an area of 0.78 km^2 at an elevation of approximately 2700 m. It lies at 41.86° North and 111.50° West. The TW Daniel Experimental Forest is on the divide of the watershed that contributes to the Logan River and Bear Lake. Average annual precipitation is about 950 mm of which about 80% is snow. The maximum snow depth can reach 5 m in the area where snow drifts occur. Vegetation is comprised of deciduous forest (Aspen), coniferous forest (Engelmann spruce and subalpine fir), open meadows consisting of a mixture of grasses and forbs, and shrub areas dominated by sagebrush.

Instrumentation was installed starting 2006 to monitor weather and snow within four different vegetation classes: grass, shrubs, coniferous forest, and deciduous forest; and includes twelve weather station towers (three replicates in each vegetation class), one central tower (in shrub area) with more comprehensive radiation instrumentation and one SNOTEL station in a clearing within the coniferous forest. The following automated data were collected:

- Continuous measurements of snow depth (Judd communications depth sensor) at each of the twelve stations.
- Continuous measurements of weather: temperature (Vaisala HMP50); wind (Met One, 014A); net radiation, (Kipp & Zonin NR-Lite); humidity, (Vaisala HMP50) at one station in each vegetation class.
- Four separate radiation components: downward and upward shortwave and long wave (Hukseflux, NR01 4-way radiometer) and snow surface temperature (Apogee Instrument, IRR-PN) at the centralized weather station.
- The standard suite of SNOTEL observations at the adjacent SNOTEL site, from which we used precipitation.

Field observations roughly every two weeks for three winters (2006/7 - 2008/9) comprised two snow pits: one in the shrub area and the other in a conifer clearing, and probing snow depth at multiple locations in all four vegetation classes. Within each snow pit samples were taken at 10 cm vertical intervals over the entire snow pit depth using a 250 cm^3 stainless steel cutter to derive the snow density. The density measured at the pit in the shrub area was used to represent both shrub and grass areas (open snow cover during the winter snow season because snow completely covers the shrubs), while the density measured in the conifer clearing was used to represent forested areas (both conifer and deciduous). These density values were used with the depth measurements at multiple locations to derive the snow water equivalent (SWE). Temperature was also measured at the surface and at 10 cm vertical intervals over the entire snow pit depth. These temperature measurements were used to derive the energy content of the snow. Figure 1 shows the two locations near which snow pits were dug during periodic visits.

Numbers one through twenty one are snow survey locations where the depth measurements were made across the four vegetation classes.

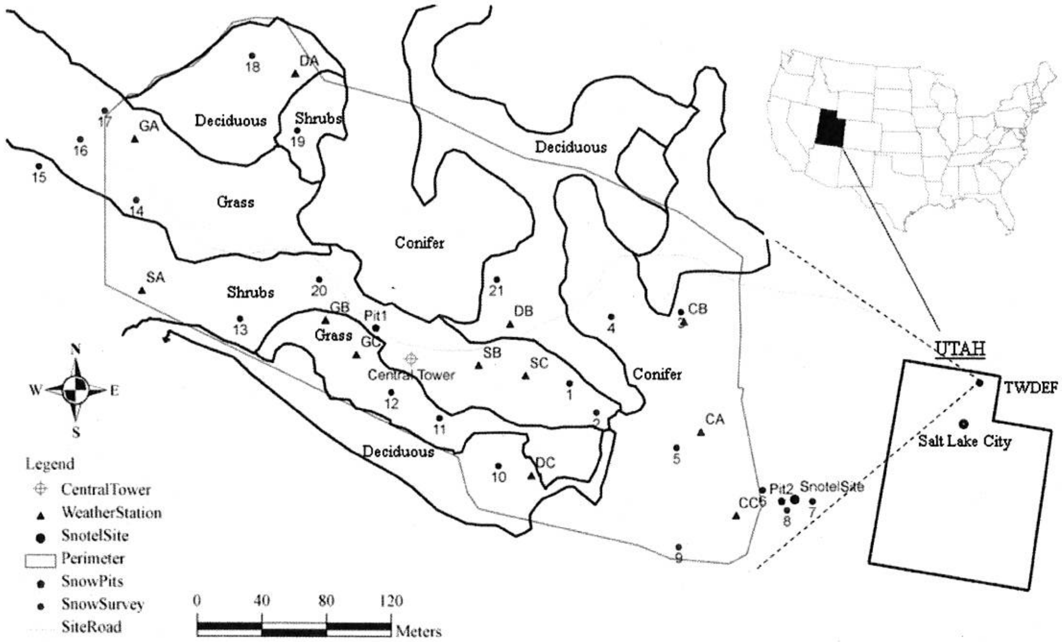

Figure 1. Site map of the TW Daniel Experimental Forest showing weather station towers, vegetation, survey points, pits and SNOTEL site.

MODEL ENHANCEMENT

Three major enhancements: i) representation of snow interception and unloading, ii) representation of the transmission of radiation through the canopy and iii) representation of the atmospheric transport of heat and water vapor between the snow on the ground, intercepted snow in the canopy and the atmosphere above, were made to the UEB model. These enhancements add one new state variable, the water equivalent of intercepted snow in the canopy, W_c (m) to characterize the canopy snow. The other three state variables in original UEB that characterize the surface snow are water equivalent of surface snow on the ground beneath the canopy, W_s(m), energy content of snow on the ground beneath the canopy, U_s (kJ m^{-2}), and the dimensionless age of snow surface used for albedo calculations. The state variable, U_s is defined relative to a reference state of water at 0 °C in the ice (solid) phase. U_s greater than zero means the snowpack (if any) is isothermal with some liquid content and U_s less than zero can be used to calculate the snowpack average temperature T_{ave}(°C). Energy content is defined as the energy content of the snowpack plus a top layer of soil with depth, D_e(m). We assume the energy content of intercepted snow in the canopy is negligible and does not need to be maintained as a separate state variable. Canopy temperature, including snow in the canopy, is assumed to adjust to maintain energy equilibrium, except when this requires canopy temperature to be greater than freezing when snow is present in the canopy, in which case the extra energy drives the melting of snow in the canopy.

The changes with time of surface energy content, U_s, surface water equivalent, W_s, and canopy water equivalent W_c, are determined by following three equations.

$$\frac{dU_s}{dt} = Q_{sns} + Q_{lns} + Q_{ps} + Q_g + Q_{hs} + Q_{es} - Q_{ms} \quad (1)$$

$$\frac{dW_s}{dt} = P_r + P_s - i + R_m + M_c - E_s - M_s \quad (2)$$

$$\frac{dW_c}{dt} = i - R_m - M_c - E_c \quad (3)$$

In these equations, energy fluxes are: 1) net sub-canopy shortwave radiation, Q_{sns}, 2) net sub-canopy longwave radiation, Q_{lns}, 3) advected heat from precipitation, Q_{ps}, 4) ground heat flux, Q_g, 5) sensible heat flux, Q_{hs}, 6) latent heat flux due to sublimation/condensation, Q_{es}, 7) advected heat removed by melt water Q_{ms}. Mass fluxes are rainfall, P_r, 2) snowfall P_s, 3) canopy interception, i, 4) mass release from the canopy, R_m, 5) melt water drip from the canopy snow, M_c, 6) melt from the surface snow, M_s, 7) sublimation from the canopy snow, E_c, 8) sublimation from the surface snow, E_s. All terms in the energy balance equation are expressed per unit of horizontal area in kJ m^{-2} hr^{-1}. All terms in the mass balance equations are expressed in m hr^{-1}.

Canopy energy balance is given by

$$Q_{snc} + Q_{lnc} + Q_{pc} + Q_{hc} + Q_{ec} - Q_{mc} = 0 \tag{4}$$

where Q_{snc} is net canopy shortwave radiation, Q_{lnc} is net canopy longwave radiation, Q_{pc} is net advected heat from precipitation to the canopy, Q_{hc} is sensible heat to the canopy, Q_{ec} is latent heat to the canopy, and Q_{mc} is advected heat removed by melt water from the canopy. This equation reflects our assumption that the energy content of intercepted snow is negligible. In this equation Q_{mc} is first set to 0 and the other terms used to solve for canopy temperature, T_c. If the result is above freezing (0 °C) and there is snow present in the canopy, then T_c is set to freezing and the resulting Q_{mc} used to determine M_c.

Details of the original UEB model formulation are given by Tarboton et al. (1995), Tarboton and Luce (1996), and You (2004). In the following sections we describe the canopy process enhancements.

<u>Transmission of Radiation through the Canopy</u>

The incoming solar radiation was partitioned into direct and diffuse components as these components penetrate the canopy separately. Partitioning was based on scattering and absorption properties of the atmosphere using the approach described by Bristow and Campbell (1984), Shuttleworth (1993), and Dingman (2002). To model the penetration of radiation through the canopy accounting for multiple scattering we used the two stream (downward and upward) approach of Monteith and Unsworth (1990). Direct beam transmittance through the canopy is given by:

$$\tau_b(L, \theta, \alpha) = e^{-k' K_b L} \tag{5}$$

This shows an exponential attenuation of light intensity based on leaf area index, L, but with the exponential decrease coefficient reduced by a factor $k' = \sqrt{1-\alpha}$ that quantifies the effect of multiple scattering. Here α is the leaf scale reflectance, $K_b = G/cos\theta$ is the non scattering attenuation coefficient that accounts for leaf orientation through geometry factor G and zenith angle θ. Strictly this approach only applies for horizontal leaves (Monteith and Unsworth 1990) but Goudriaan (1977) suggests it can be used as an approximation for other leaf orientations. We assume G is constant and use G =0.5 for spherical leaves.

The approach for diffuse beam radiation is to use (5) in each direction and integrate the components of the directional beam over the hemisphere. Assuming isotropic diffuse radiation from the sky and in the canopy results in diffuse transmittance (Nijssen and Lettenmaier, 1999):

$$\tau_d(L) = \left[(1 - k'GL)\, e^{(-k'GL)} + (k'\, GL)^2\, Ei(1,\ k'GL)\right] \tag{6}$$

where $E_i(n, x)$ is the exponential integral function.

Radiation impacting a canopy is either transmitted, reflected or absorbed. The aggregate fraction of either direct or diffuse radiation reflected from the canopy with the two stream multiple scattering approach above is given by (Monteith and Unsworth, 1990):

$$R = (1 - \tau)\frac{(1-k')}{1+k'} \tag{7}$$

where τ may be τ_b from (4) or τ_d from (6). The fraction absorbed in the canopy is obtained from the fractions transmitted and reflected by subtraction from 1.

Reflection of radiation that penetrates the canopy from the surface is calculated from surface albedo. This is assumed to be diffuse and isotropic. Multiple reflections between the canopy and surface are modeled using (7) with τ_d for the downward reflection from the canopy.

Longwave radiation originates from three possible sources: the sky, the snow surface and the canopy. Longwave radiation from each of these sources is considered to be diffuse radiation that penetrates through or is scattered by the canopy according to (6) and (7). However the scattering of longwave radiation is much less than that of shortwave radiation because the leaf scale reflectance for longwave, $\alpha = 1 - \varepsilon$, is very close to 0, where ε is emissivity. Longwave radiation emitted by the canopy is calculated as $\varepsilon\sigma T^4(1 - \tau_d)$, where σ is the Stefan–Boltzmann constant and T is the air temperature in Kelvin. Multiple reflections between canopy and the surface are considered in same manner for longwave as for shortwave radiation, but with different reflectance.

Turbulent Flux Transfer Processes in Canopy

A two-source flux model treating the canopy and the underlying snow as two horizontal layers was developed. The energy balance was solved for each layer, and the transfer of mass (latent heat) and heat (sensible heat) to and from the canopy and underlying snow were estimated separately using the concept of flux proportional to temperature and vapor pressure gradients. Three resistances were calculated to model fluxes between (1) the surface and air in the canopy (within canopy), (2) air in the canopy and air above (above canopy), and (3) canopy and air in the canopy (bulk leaf resistance) respectively (Figure 2). The height for separation of within and above canopy resistances was taken as the level of the effective momentum sink at $d + z_{oc}$ where d is displacement height and z_{oc} is the roughness length for the top of canopy boundary layer estimated from vegetation height, tree properties and L following Shaw and Periera (1982). K-theory was used to calculate the first two resistances from an assumed wind profile comprised of a logarithmic part above the canopy followed by exponential part within the canopy and logarithmic part near the surface (e.g. Shuttleworth and Gurney, 1990; Dolman, 1993; Koivusalo, 2002). Bulk leaf boundary layer resistance was calculated based on leaf dimension and leaf area distribution (e.g. Jones, 1992; Choudhury and Monteith, 1988). The within canopy resistance was corrected for atmospheric stability (Storck 2000, Essery et al. 2003). In this approach sensible heat and latent heat fluxes are expressed as:

$$Q_{hs} = \frac{\rho_a C_p (T_{ac} - T_{ss})}{R_c^*},\ Q_{hc} = \frac{\rho_a C_p (T_{ac} - T_c)}{R_l},\ Q_h = Q_{hs} + Q_{hc} = \frac{\rho_a C_p (T_a - T_{ac})}{R_a} \tag{8}$$

$$Q_{es} = \frac{1}{R_c^*}\frac{h_v\, 0.622}{R_d T_{ac}}\left(e_{ac} - e_s(T_{ss})\right),\ Q_{ec} = \frac{1}{R_l}\frac{h_v\, 0.622}{R_d T_{ac}}\left(e_{ac} - e_s(T_c)\right),$$

$$Q_e = Q_{ec} + Q_{es} = \frac{1}{R_l}\frac{h_v\, 0.622}{R_d T_{ac}}\left(e_a - e_{ac}\right) \tag{9}$$

where Q_h, Q_{hc}, Q_{hs} are sensible heat fluxes (positive downward) from the atmosphere to canopy air, canopy air to canopy surface and canopy air to ground surface respectively. Q_e, Q_{ec}, Q_{es} are latent heat fluxes (positive downward) from the atmosphere to canopy air, canopy air to canopy surface and canopy air to ground surface respectively. T_a, T_{ac}, T_{ss} and T_c are air temperature above the canopy, within the canopy, surface temperature of snow on the ground and in the canopy respectively. e_a, e_{ac}, $e_s(T_{ss})$ and $e_s(T_c)$ are actual vapor pressure above the canopy, within the canopy, saturated vapor pressure of the snow surface on the ground and within the canopy respectively. ρ_a is air density, C_p is air specific heat capacity (1.005 kJ kg^{-1} °C^{-1}), h_v the latent heat of sublimation (2834 kJ kg^{-1}) and R_d is the dry gas constant (287 J kg^{-1} K^{-1}). R_c^* is the aerodynamic resistance to heat and vapor transport (hr m^{-1}) between surface and air in the canopy corrected for atmospheric stability, R_l is bulk leaf boundary layer resistance. R_a is the aerodynamic resistance between air in the canopy and air above the canopy. The resistances for heat and mass transfer are assumed to be equal. Energy conservation for sensible and latent heat expressed in (7) and (8) as $Q_h = Q_{hs} + Q_{hc}$ and $Q_e = Q_{ec} + Q_{es}$ facilitates the evaluation T_{ac} and e_{ac} given T_a and e_a as inputs and once T_{ss} and T_c are solved using the energy balance at surface and within the canopy.

Figure 2 illustrates wind profiles and the resistances calculated using these profiles. The model inputs are wind speed u_m at height z_m above the canopy. Assuming log, followed by exponential, followed by log wind profiles, wind speeds u_h at canopy height, h, u_{ms}at height z_{ms}=2 m above the surface and at points in between are determined. The diffusivity, K, is determined from the wind speed gradient and used to evaluate resistances (e.g. Shuttleworth and Gurney, 1990; Dolman, 1993; Koivusalo, 2002). Specifically $R_a = \int_{d+z_{oc}}^{z_m} \frac{dz}{K}$ and $R_c =$

$\int_{z_{os}}^{d+z_{oc}} \frac{dz}{K}$. Bulk leaf boundary layer resistance was calculated following Jones (1992) and Choudhury and Monteith (1988) using wind speed at $d + z_{oc}$.

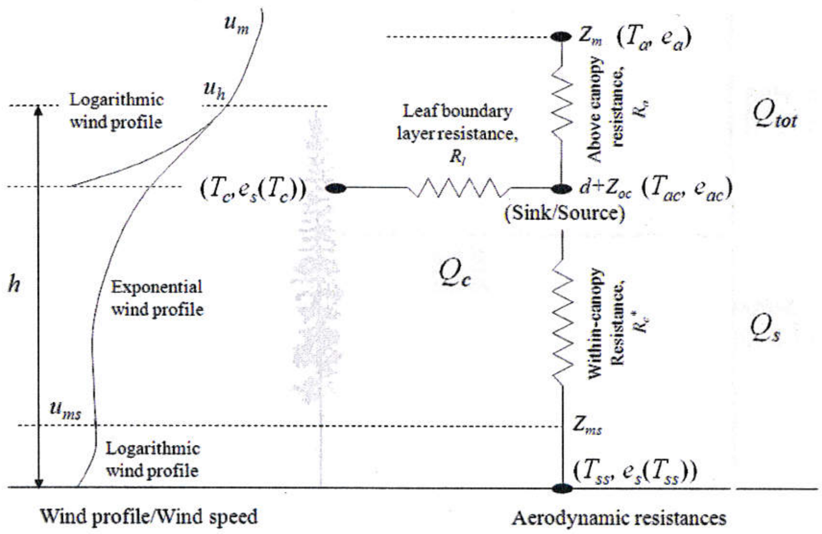

Figure 2. Energy exchange between snow at ground, in canopy and the atmosphere.

Snow Interception and Unloading Processes

The rate of interception was modeled as a fraction of the rate of precipitation using

$$i = k\ (1 - \frac{W_c}{I_{max}})p \tag{10}$$

where W_c is the canopy water equivalent interception load in the canopy, I_{max}, is the canopy interception capacity, p the precipitation rate, i the interception rate and k the canopy coverage fraction. This is based on the interception models of Aston (1979) and Hedstrom and Pomeroy (1998) formulated to be continuous rather than event based. W_c evolves according to equation (3), which in addition to i, requires R_m, M_c, and E_c to be evaluated.

Interception sublimation loss was evaluated based on Q_{ec} determined above, equation (9). The mass release of intercepted snow, R_m is modeled as an exponential function of time (Hedstrom and Pomeroy 1998), and melt water drip, M_c, is quantified based on canopy energy balance, using energy fluxes (radiation, sensible and latent heat) determined above.

Maximum interception storage capacity, I_{max} is obtained as $I_{max} = I_b L$, where I_b (kg m^{-2}) is the per unit of leaf area maximum snow load and L is leaf area index. Schmidt and Gluns (1991) made extensive field measurements of interception capacity and reported reference $\overline{I_b}$ values of 6.6 and 5.9 kg m^{-2} for pine and spruce trees respectively. They also suggested an adjustment for snow density:

$$I_b = \overline{I_b}\ (0.27 + \frac{46}{\rho_s}) \tag{11}$$

where, ρ_s is the fresh snow density (kg m^{-3}) estimated based on air temperature (e.g. Hedstrom and Pomeroy, 1998; Schmidt and Gluns, 1991; U.S. Army Corps of Engineers, 1956). Equation (11) was used with leaf area index to calculate I_{max} in our model.

RESULTS

Direct Observations

Maximum SWE determined from the probed snow depths and pit snow densities for each of the vegetation classes show generally greater accumulations in open (grass and shrubs) as compared to forest (deciduous/coniferous) areas (Figure 3) by about 10 to 20%. SWE values at survey points 14, 15, 16 and 17 (Figure 1) are anomalously large because of a snow drift that accumulates behind the ridge on the west side of the site. SWE at these points was therefore aggregated separately as "Drift" (Figure 3) and not included in the shrubs and grass SWE values. Even though accumulations in forest areas were less, they tended to ablate more slowly and persist longer than the snow in the open areas. Small differences between SWE in the coniferous and deciduous forest areas are notable, with higher accumulation and more rapid ablation in deciduous forest compared to coniferous forest. Lower accumulation in the forested areas is attributed to interception and subsequent sublimation and redistribution of intercepted snow by wind. Lower melt rates in the forest are attributed to reduced wind speed and radiation attenuation by the forest canopy.

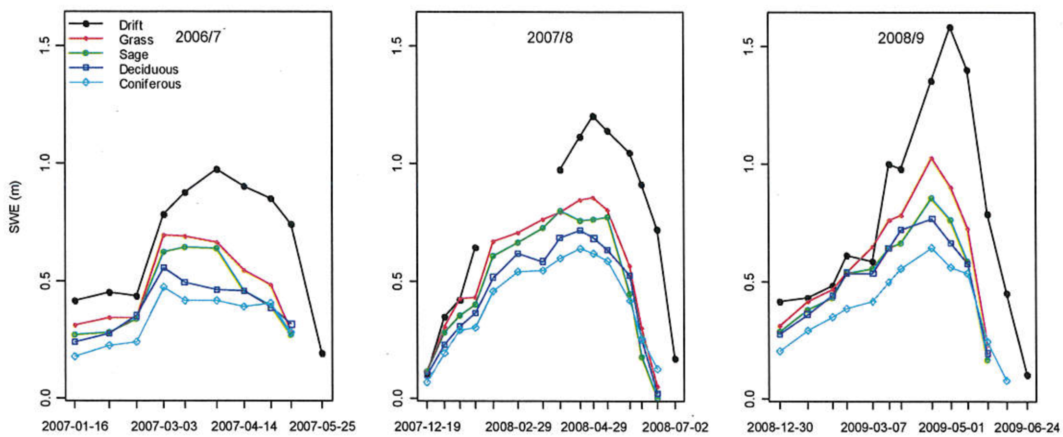

Figure 3. Snow water equivalent observed in shrubs, grass, coniferous forest, deciduous forest and drift area during three winters.

Model Evaluation

The enhanced model was run for the period of January 2008 to July 2008, and December 2008 to July 2009 using the hourly meteorological inputs (precipitation, temperature, wind speed and relative humidity) to evaluate the snow processes in open, deciduous and coniferous forest. Errors in the input meteorological data precluded us from running the model for the 2006/2007 winter. Input precipitation data was taken from the SNOTEL site (Figure 1) and the other meteorological input data were obtained from the shrubs B (SB) open site. The model predicts the snow processes in both open and forest areas with this meteorological input, assuming for forest areas that the open site meteorological variables are representative of conditions at a height of 2 m above the forest canopy. The model predicted the SWE, snow surface temperature, snow average temperature, canopy wind speed, radiation, energy fluxes, interception for both open and forest areas. Model performance was assessed by comparing some of these results with the field observed data. Slope and aspect that significantly affects the radiation input to the surface were determined from a high resolution DEM obtained from LIDAR. Leaf area index, tree height and canopy coverage were determined based on field observation. Other model parameters follow the original UEB model (Tarboton and Luce, 1996; You, 2004).

The open model runs were conducted using parameters for survey point 1 (Figure 1), selected because it was deemed to be the least impacted by drifting or scouring due to wind. The deciduous and coniferous forest model runs were conducted using parameters for locations DB and CA respectively (Figure 1) as these are the instrument towers where below canopy radiation and meteorology was also measured. This data, which was not used to drive the model, provides a way to evaluate the canopy process parameterizations that have been introduced.

Net Radiation

The observed net radiation beneath the canopy was compared with the modeled values calculated based on transmission through and attenuation by the canopy as described above, aggregated to daily time scale (Figure 4). As expected, net radiation beneath the coniferous canopy is less than beneath the deciduous canopy which is also generally less than in the open. The model generally represents these effects although it does have a tendency to over predict the net radiation particularly in mid winter for the deciduous and coniferous locations. The model shows relatively good agreement with observations during spring, which is important for calculating melt.

The model overprediction of net radiation beneath the coniferous canopy during the early winter could due to many factors. Snow has a tendency to collect on the upper part of the net radiometer that may bias the observations. The radiation transmission model has a number of simplifications and does not represent canopy architecture, leaf orientation and layering effects. There are also uncertainties associated with the leaf level reflectances that were taken from the literature and estimates of leaf area index. Given these uncertainties, the degree of agreement in Figure 4 is satisfying.

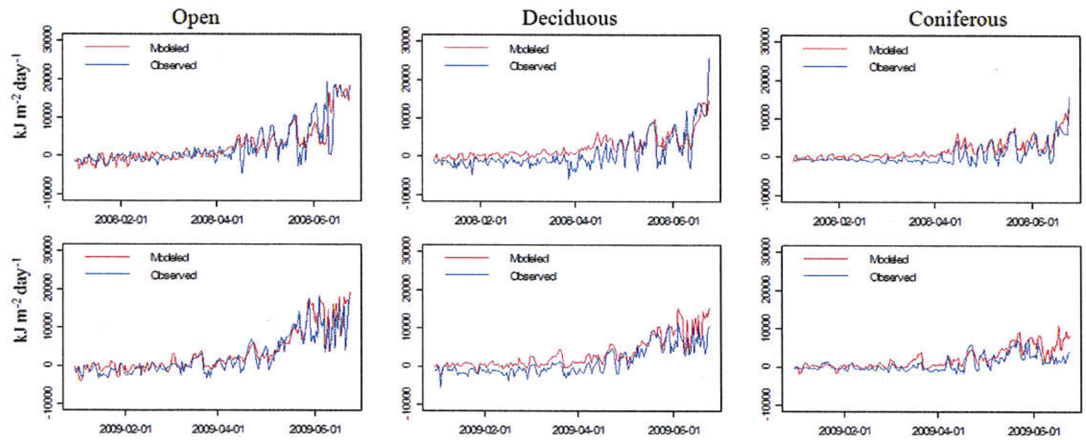

Figure 4. Net radiation: observed and modeled, in open and beneath the deciduous and coniferous forest canopy.

Wind

The model represents the wind profile through the canopy using separate log, exponential and then log profiles above, in and below the canopy (Figure 2), with the exponential attenuation of wind speed following the model from Cionco (1972). Inputs to the modeled wind speed calculation comprise the measured wind speed in the open assumed to be equivalent to the above canopy wind, and the canopy parameters, leaf area index and height. The modeled wind speed at 2 m above the surface was compared to measured wind speed beneath the canopy aggregated to a daily time scale (Figure 5). These comparisons indicate that the greater density of coniferous forest canopies, reflected by their higher leaf area index result in lower beneath canopy wind speeds, and that the model parameterization is able to capture this effect.

SWE

The integrated effect of all model inputs and processes is reflected in its simulation of SWE on the ground in the open and underneath deciduous and forested canopies (Figure 6). Observed SWE in Figure 6 for the open comparison is at location 1 (Figure 1) chosen because it is deemed to be least impacted by scour or drifting. Observed SWE beneath deciduous and coniferous forest canopies is the average of all point measurements in these vegetation classes. The model was initialized with SWE equal to the first observed value shown in these figures. The greater accumulation in open areas is evident in the observations and captured by the model, although this is partly due to the initialization. The more rapid ablation in the open areas is evident in the observations and captured by the model, reflecting the model's capability to, in aggregate, represent the processes driving snow melt in open and forested areas, with appropriate sensitivity to forest parameters.

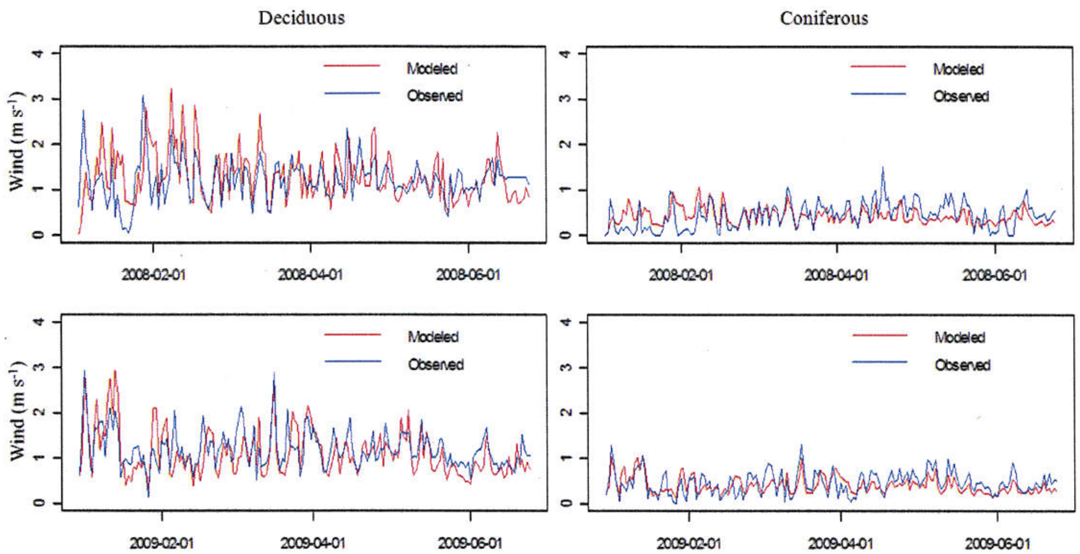

Figure 5. Wind speed: observed and modeled beneath the deciduous and coniferous forest canopy.

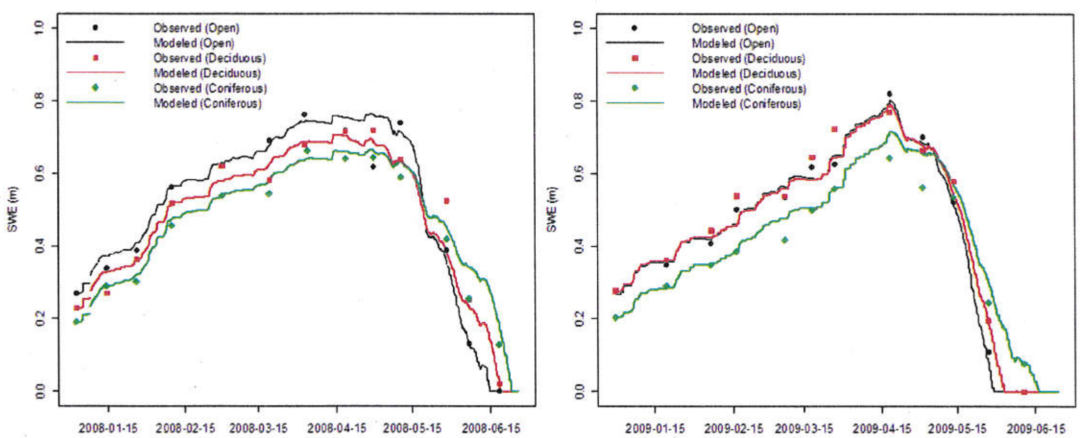

Figure 6. SWE comparison across different vegetation classes.

DISCUSSION AND CONCLUSIONS

To better understand the snow processes in forested areas the UEB model has been enhanced to include, i) interception process, ii) canopy radiation transmission process, and iii) turbulent flux transmission process. Observations in four vegetation classes were used to evaluate aspects of these new model parameterizations. The enhanced UEB model reproduced the higher accumulation in open site and lower accumulation in forest areas consistent with observations. The model was also able to capture the differences in ablation between open and forest areas and the differences between coniferous and deciduous forest.

The observed precipitation accumulated during the 2007-08 and 2008-09 simulation periods was 668 and 734 mm respectively. For both of these periods, the model simulated about 37% of precipitation intercepted by coniferous forest, out of which 17 % sublimated, 24% unloaded as a mass and 59% unloaded as melt water from the canopy. In deciduous forest about 22% of precipitation was simulated as intercepted, out of which 16 % sublimated, 15% unloaded as a mass and 69% unloaded as melt water from the canopy. Snow that unloads from the canopy as mass or melt water adds to the below canopy snowpack, while the sublimation is a loss from the water resources perspective. However this is offset by lower amounts of sublimation from the surface when a canopy is present. In our simulations there was greater total sublimation (canopy and surface) from the forested areas in the first half and middle of the simulation period. This seems to be responsible for the lower accumulations in the forest. However during the latter part of the simulations there is little intercepted snow in the canopy (and hence little canopy sublimation) suppressing sublimation from the forested area. This is part of an overall reduction in energy fluxes beneath the forest. These effects offset each other to that the net loss to sublimation was, in this specific simulation, roughly equivalent between open and forested areas. Hence the surface water input was also roughly equivalent. However the more rapid surface water input from open areas provides greater opportunity for surface runoff and occurs earlier, while the slower surface water input from forested areas persists later into the season, sustaining streamflow longer, but is also more subject to infiltration into the soil and uptake and transpiration by vegetation which may result in reduced streamflow.

This work has evaluated net radiation, sub canopy wind and overall SWE aspects of the enhanced model. Further evaluation is required to examine other aspects, specifically the sublimation and interception components. Further evaluation is also required in different settings. Extension of the model over larger areas to evaluate the watershed scale impacts of vegetation distribution should also be pursued.

ACKNOWLEDGEMENTS

This research was supported by the USDA-CREES Utah drought management project award number 2008-34552-19042.

REFERENCES

Anderson, E. A. 1976. A Point Energy and Mass Balance Model of a Snow Cover. NOAA Technical report NWS 19, U.S. Department of Commerce,

Andreadis, K. M., P. Storck, and D. P. Lettenmaier. 2009. Modeling snow accumulation and ablation processes in forested environments. Water Resources Research, 45(5): W05429. http://dx.doi.org/10.1029/2008WR007042

Aston, A. R. 1979. Rainfall interception by eight small trees. Journal of Hydrology 42: 383-396

Bonan, G. B. 1991. A Biophysical Surface Energy Budget Analysis of Soil Temperature in the Boreal Forests of Interior Alaska. Water Resources Research, 27(5): 767-781

Bristow, K. L. and G. S. Campbell. 1984. On the Relationship Between Incoming Solar Radiation and the Daily Maximum and Minimum Temperature. Agricultural and Forest Meteorology, 31: 159-166

Choudhury, B. J. and J. L. Monteith. 1988. A four-layer model for the heat budget of humogeneous land surface. Quarterly Journal of the Royal Meteorological Society, 114(1988): 373-398

Cionco, R. M. 1972. A Wind Profile for Canopy Flow. Boundary-Layer Meteorology, 3: 255-263

Dingman, S. L. 2002. Physical Hydrology. 2nd Edition, Prentice Hall, 646 p.

Dolman, A. J. 1993. A multiple- source land surface energy balance model use in general circulation models. Agric. For. Meteorol., 65(1-2): 21-45

Ellis, C. R. and J. W. Pomeroy 2007. Estimating sub-canopy shortwave irradiance to melting snow on forested slopes. Hydrological Processes, 21(19): 2581-2593. http://dx.doi.org/10.1002/hyp.6794

Essery, R., J. Pomeroy, J. Parviainen, and P. Storck. 2003. Sublimation of Snow from Coniferous Forests in a Climate Model. Journal of Climate, 16(1 June 2003): 1855-1864

Flerchinger, G. N., W. P. Kustas, and M. A. Weltz. 1998. Simulating Surface Energy Fluxes and Radiometric Surface Temperatures for Two Arid Vegetation Communities using the SHAW Model. Journal of Applied Meteorology, 37(5): 449-460

Goudriaan, J. 1977. Crop meteorology: A Simulation Study, Simulation monographs,. Cent. for Agric. Publ. and Doc., Wageningen, Neth.

Hedstrom, N. R. and J. W. Pomeroy. 1998. Measurements and modelling of snow interception in the boreal forest. Hydrological Processes, 12(10-11): 1611-1625

Jones, H. G. 1992. Plants and microclimates. 2nd Edition, Cambridge university press, New York, 63-64 pp.

Jordan, R. 1991. A one-dimensional temperature model for a snow cover. Technical documentation for SNTHERM.89, special technical report 91-16, US Army CRREL,

Koivusalo, H. 2002. Process-Oriented Investigation of Snow Accumulation, Snowmelt and Runoff Generation in Forested Sites in Finland. PhD Thesis, Helisinki University of Technology Water Resources Publication.

Lundberg, A., I. Calder and R. Harding. 1998. Evaporation of intercepted snow: measurement and modelling. Journal of Hydrology, 206: 151-163

Lundberg, A. and S. Halldin. 1994. Evaporation of intercepted snow: analysis of governing factors. Water Resouces Research, 30(9): 2587-2598

Mackay, M. D. and P. A. Barlett. 2006. Estimating canopy snow unloading timescales from daily observations of albedo and precipitation. Geophysical Research Letters, 33: L19405

Marks, D., J. Dozier, and R. E. Davis. 1992. Climate and Energy Exchange at the Snow Surface in the Alpine Region of the Sierra Nevada, I: Meteorological Measurements and Monitoring, II: Snowcover Energy Balance. Water Resources Research, 28(11): 3029-3054

Marks, D., J. Kimball, D. Tingley, and T. Link. 1998. The Sensitivity of Snowmelt Processes to Climate Conditions and Forest Cover During Rain-on-snow: A Study of the 1996 Pacific Northwest Flood. Hydrological Processes, 12: 1569-1587

Marks, D., M. Reba, J. Pomeroy, T. Link, A. Winstral, G. Flerchinger, and K. Elder. 2008. Comparing Simulated and Measured Sensible and Latent Heat Fluxes over Snow under a Pine Canopy to Improve an Energy Balance Snowmelt Model. Journal of Hydrometeorology, 9(6): 1505-1522. http://dx.doi.org/10.1175/2008JHM874.1.

Molotch, N. P., P. D. Blanken, M. W. Williams, A. A. Turnipsesd, R. K.Monson, and S. A. Marguilis. 2007. Estimating sublimation of intercepted and sub-canopy snow using eddy covariance system. Hydrological Processes, 21(2007): 1567-1575

Monteith, J. L. and M. H. Unsworth. 1990. Principles of Environmental Physics. 2nd Edition, London.

Nakai, Y., T. Sakamoto, T. Terajima, K. Kitamura, and T. Shirai. 1999. The effect of canopy-snow on the energy balance above a coniferous forest. Hydrological Processes, 13: 2371-2382

Nijssen, B. and D. P. Lettenmaier. 1999. A simplified approach for predicting shortwave radiation transfer through boreal forest canopies. Journal of Geophysical Research, 104(D22): 27859-27868

Norman, J. M. 1979. Modeling the Complete Crop Canopy In B. J. Barfield and J. F. Gerber (Ed.), Modification of the Arial Environment of Plants. American Society of Agricultural Engineers, St. Joseph, Michigan, pp. 249-277.

Pomeroy, J. W., J. Parviainen, N. Hedstrom, and D. M. Gray. 1998. Coupled modelling of forest snow interception and sublimation. Hydrological Processes, 12(15): 2317-2337

Price, A. G. and T. Dunne. 1976. Energy balance computations of snowmelt in a subarctic area. Water Resources Research, 12(4): 686-694

Sanchez, J. K., V. Caselles, R. Niclos, C. Coll, and W. P. Kustas. 2009. Estimating energy balance fluxes above a borel forest from radiametric temperature observations. Agricultural and Forest Meteorology, 149: 1037-1049

Schmidt, R. A. and D. R. Gluns. 1991. Snowfall Interception on Branches of Three Conifer Species. Canadian Journal of Forest Resources, 21: 1262-1269

Shaw, R. H. and A. R. Periera. 1982. Aerodynamic roughness of a plant canopy: A numerical experiment. Agric. Meteorol., 26: 51-65

Shuttleworth, W. J. 1993. Evaporation. In D. R. Maidment (Ed.), Handbook of Hydrology, Chapter 4. McGraw-Hill, New York.

Shuttleworth, W. J. and R. J. Gurney. 1990. The theroretical relationship between foliage temperature and canopy resistance in sparse crops. Q. J. R. Meteorol.Soc., 116: 497-519

Shuttleworth, W. J. and J. S. Wallace. 1985. Evaporation from sparse crops-an energy combination theory. Quarterly Journal of the Royal Meteorological Society, 111(1985): 839-855

Storck, P. 2000. Trees, snow and flooding: An investigation of forest canopy effects on snow accumulation and melt at the plot and watershed scales in the Pacific Northwest. Department of Civil and Environmental Engineering, University of Washington,

Storck, P., D. P. Lettenmaier, and S. M. Bolton. 2002. Measurement of snow interception and canopy effects on snow accumulation and melt in a mountainous maritime climate, Oregon, United States. Water Resources Research, 38(11): -. http://dx.doi.org/10.1029/2002WR001281

Tarboton, D. G., T. G. Chowdhury, and T. H. Jackson. 1995. A Spatially Distributed Energy Balance Snowmelt Model. In K. A. Tonnessen, M. W. Williams and M. Tranter (Ed.), Proceedings of a Boulder Symposium, July 3-14, IAHS Publ. no. 228, pp. 141-155.

Tarboton, D. G. and C. H. Luce. 1996. Utah Energy Balance Snow Accumulation and Melt Model (UEB). Computer model technical description and users guide, Utah Water Research Laboratory and USDA Forest Service Intermountain Research Station (http://www.engineering.usu.edu/dtarb/),

U.S. Army Corps of Engineers. 1956. Snow Hydrology, Summary report of the Snow Investigations. U.S. Army Corps of Engineers, North Pacific Division, Portland, Oregon,

Wigmosta, M. S., L. W. Vail, and D. P. Lettenmaier. 1994. A Distributed Hydrology-Vegetation Model for Complex Terrain. Water Resources Research, 30(6): 1665-1679

You, J. 2004. Snow Hydrology: The Parameterization of Subgrid Processes within a Physically Based Snow Energy and Mass Balance Model. PhD Thesis, Utah State University.